Bioprocess and Biosystems Engineering (2024) 47:697–712
https://doi.org/10.1007/s00449-024-02999-1

RESEARCH PAPER

Kinetic modeling and optimization of the mono- and diglycerides synthesis mediated by the lipase Lipozyme® TL 100 L immobilized on clayey support

George F. Finco[1] · Edson A. da Silva[1] · Fernando Palú[1] · Márcia R. F. Klen[1] · Karina G. Fiametti[2] · João H. C. Wancura[3] · J. Vladimir Oliveira[4]

Received: 30 October 2023 / Accepted: 12 March 2024 / Published online: 27 March 2024

Abstract

Mono- and diglycerides play a crucial role in the food industry as multifunctional food additives and emulsifiers. Their importance stems from their unique properties, which allow them to improve the quality, texture, and stability of various food products. Here, results of the kinetic modeling of the mono- and diglycerides synthesis mediated by the lipase Lipozyme® TL 100 L immobilized on the clayey support Spectrogel® type C are reported. The support was characterized by TEM, SEM, and FTIR. Firstly, the influence of pH and lipase load on the immobilization process was analyzed, resulting in an enzymatic activity of 93.2 ± 0.7 U g^{-1} under optimized conditions (170.9 U g^{-1} of lipase and pH of 7.1). Afterward, the effects of reaction temperature and concentration of immobilized biocatalyst in the feedstock conversion were evaluated. At optimized parameters, a triglycerides conversion of 97% was obtained at 36.5 °C, 7.9 vol.% of enzyme, a glycerol to feedstock molar ratio of 2:1, and 2 h. The optimized conditions were used to determine the kinetic constants of the elementary reactions involved in the glycerolysis, where a fit superior to 0.99 was achieved between experimental values and predicted data.

Keywords Monoacylglycerols · Diacylglycerol · Triacylglycerol · Biocatalysis · Emulsifier

Introduction

Monoglycerides (MAGs) are a class of lipids that can be naturally occurring in certain foods or produced synthetically for distinct purposes. In food, these compounds are typically applied as emulsifiers [1]. Due to their structure, MAGs have both hydrophilic and hydrophobic properties, making them effective in stabilizing emulsions [2]. This property is particularly useful in food manufacturing to improve the texture, consistency, and shelf-life of products [3]. Contextually, the MAGs were considered safe for consumption, where regulatory authorities such as the *United States Food and Drug Administration* (FDA) have approved their use in food and pharmaceutical products [4, 5]. Similar to MAGs, diglycerides (DAGs) are also commonly employed in the food industry as emulsifiers [6, 7]. Their hydrophilic and hydrophobic properties allow them to interact with both water and oil-based substances, aiding in the mixing and

✉ João H. C. Wancura
jhwancura@gmail.com

George F. Finco
georgefernando.f@hotmail.com

Edson A. da Silva
edsondeq@hotmail.com

Fernando Palú
fernando.palu@unioeste.br

Márcia R. F. Klen
fagundes.klen@gmail.com

Karina G. Fiametti
karinafiametti@utfpr.edu.br

J. Vladimir Oliveira
jose.vladimir@ufsc.br

1 Department of Chemical Engineering, Western State University of Paraná, Toledo, PR, Brazil

2 Department of Bioprocess and Biotechnology Engineering, Federal Technological University of Paraná, Toledo, PR, Brazil

3 Laboratory of Biomass and Biofuels (L2B), Federal University of Santa Maria, Santa Maria, RS 97105-900, Brazil

4 Department of Chemical and Food Engineering, Federal University of Santa Catarina, Florianópolis, SC, Brazil

stabilization of emulsions [8]. Moreover, DAGs can act to combat cholesterol, prevent obesity, and reduce body fat accumulation, where their consumption may be beneficial for the reduction of cardiovascular diseases [9].

MAGs and DAGs can be synthetically produced through different methods, including the reaction of glycerol (GLY) with fatty acids via esterification and hydrolysis of triglycerides (TAGs), breaking down the ester chain into their constituent fatty acids and glycerol molecules [10]. Industrially, the production of MAGs and DAGs is conducted from the chemical glycerolysis of TAGs (a process usually accomplished at temperatures near 200 °C and catalyzed by an alkaline catalyst), where typically a mixture composed of 50 wt% of MAGs, 40 wt% of DAGs, and 10 wt% of TAGs is obtained [11, 12]. As a milder alternative, recent research has evaluated the enzymatic catalysis of the glycerolysis reaction using lipases (EC 3.1.1.3 triacylglycerol hydrolases) immobilized in polymer supports as process catalysts [13–15], where in addition to the energy demand of the process being substantially lower than the chemical process, the high selectivity of the biocatalysts prevents the occurrence of secondary reactions [16–18].

Among the several materials suitable to be applied in the enzymes' immobilization, clayey materials offer several advantages compared to other types of solid supports such as high surface area; porosity that facilitates the substrate's diffusion and reaction products, ensuring good accessibility to the immobilized enzyme; stability, "shielding" them from harsh reaction conditions and stabilizing its structure; ease of preparation; environmental friendliness; and versatility. Particularly, organophilic clays are modified to have an affinity for organic solvents and hydrophobic compounds. This property allows the carrier to interact favorably with hydrophobic regions of enzymes [19]. By utilizing hydrophobic interactions, organophilic clays can immobilize enzymes more effectively, especially those with hydrophobic active sites or hydrophobic regions critical for enzyme–substrate interactions [20]. The organophilic clay can also act as a protective matrix for the enzyme, preventing its denaturation or deactivation in organic solvent environments as well as can tolerate variations in temperature and pH, allowing the customization of reaction conditions to suit specific enzyme requirements [21]. Even with these advantages, the use of clayey compounds to immobilize lipases destined to catalyze glycerolysis reactions for the synthesis of MAG and DAG is still a little explored subject.

The use of immobilized lipases in an enzymatic process offers advantages such as reusability, enhanced stability, improved substrate accessibility, simplified separation, and enhanced productivity, making them highly valuable for various industrial applications [22, 23]. However, particularly in enzymatic glycerolysis reactions, glycerol may accumulate on the surface of the biocatalyst, impairing the interaction between substrate × enzyme, which may lead to a decrease in reaction efficiency, since glycerol would act as a competitive inhibitor of the enzyme [24]. Thus, it is usually necessary to use a smaller amount of the input in the reaction or even employ a co-solvent in the medium [5]. Anyway, it is necessary to evaluate the other parameters involved in the process that direct the reaction to the maximum conversion of the feedstock, in addition to understanding how the complex kinetic of the enzymatic reaction occurs in this system.

In this context, this work reports experimental data for the synthesis of MAGs and DAGs by enzymatic glycerolysis mediated by the lipase Lipozyme® TL 100L immobilized on the organo-clay support Spectrogel® type C. Even with the clear advantages, the use of clayey compounds to immobilize lipases destined to catalyze glycerolysis reactions for the specific synthesis of MAG and DAG—as well as kinetic information—is still a little explored subject. Furthermore, data related to the characterization of the organo-clay support mentioned are even more scarce, where the data presented in this paper aim to fill a current scientific gap. Specifically, two statistical designs were considered to evaluate the best conditions to be used in the enzyme immobilization step as well as in the glycerolysis reaction. Kinetic data for the elementary reactions involved in the process as well as the characterization of the clayey material are also presented.

Materials and methods

Inputs and chemicals

As raw material, refined olive oil (ROO, Oliva de Los Andes Premium, 0.4 wt% of acidity, 0.13 wt% of moisture, 75.3 wt% of oleic acid, 11.7 wt% of linoleic acid, 8.7 wt% monopalmitic acid, 2.9 wt% of dilinoleic acid, and 863.4 g mol^{-1}) was purchased from a local market. Glycerol, *n*-butanol, *n*-hexane, citrate phosphate, sodium phosphate, sodium hydroxide (NaOH), acetone, ethanol (all analytical grade) as well as the surfactant Tween 80 (T80, analytical grade) were purchased from Dinamica (São Paulo, Brazil). As the catalyst, the soluble lipase Lipozyme® TL 100L was a gift from Novozymes Latin America (Araucaria, Brazil), produced from the fungus *Thermomyces lanuginosus*, with a nominal enzymatic activity of 100 LCLU·g^{-1}. From the SpectroChem Company (Joinville, Brazil), it was purchased the commercial organo-clay adsorbent Spectrogel® type C (granulometry of 0.655 mm and pretreated with a quaternary salt), an organophilic bentonite functionalized with dialkyl dimethylammonium. From the Sigma-Aldrich (São Paulo Brazil), all the HPLC standards were obtained: dilinoleic acid (98% of purity), linoleic acid (97% of purity), monopalmitic acid (> 99% of purity), acid oleic acid (> 99% of purity), trilinoleic glycerol (98% of purity) and trioleic

glycerol (> 99% of purity) as well as the solvents acetone and acetonitrile (chromatographic grade).

Microemulsions

To increase the contact area between the enzyme and the substrates, microemulsions were used. Microemulsions provide higher mutual miscibility of the GLY in nonpolar solvents, improving the interaction with the surface area of the biocatalyst, where the TAG molecule breaks down to form MAG and DAG [4].

Aiming to select an adequate proportion between raw material × surfactant × water that generates a stable microemulsion to be used in the glycerolysis reactions, different ratios of these inputs were evaluated for distinct volumetric ratios between GLY and ROO (1:1, 2:1, 3:1, 1:2 and 1:3), as presented in Table S1 (supplementary material) and following the methodology described by Finco et al. [13]. The microemulsions were considered stable when visually it was identified as a homogeneous and clear medium after 48 h of storage at 23 ± 1 °C. The stable microemulsions were subjected to glycerolysis tests at 45 °C, a volumetric ratio between GLY:ROO of 2:1, 7.5 vol.% of immobilized lipase and 2 h [25] to preliminarily evaluate the feedstock conversion into MAGs and DAGs and thus define the range of variables to be analyzed in the statistical design described in section "Enzymatic glycerolysis". Table S1 describes in detail the amount of each reagent used in these preliminary tests.

Enzyme immobilization

In the immobilization procedure of the Lipozyme® TL 100L lipase in the organo-clay adsorbent Spectrogel® type C, a central composite rotational design was used (CCRD, $2^k + 2{\cdot}k$ with three repetitions at the central point) to investigate the influence of the pH in the medium (x_1, ranging from 3.3 to 10.7 with center point of 7.0) and lipase load (x_2, ranging from 64 to 195 U g^{-1}, with center point in 130 U g^{-1}) in the catalytic activity of the enzyme after biocatalyst immobilization (dependent variable, Y, U·g^{-1}). Such ranges were defined according to data reported by Zhu et al. [26] and Dizge et al. [27], where for all tests, 24 h and 35 °C were set [28]. As buffer solutions, citrate phosphate (pH 5.0), sodium phosphate (pH 7.0), and sodium phosphate adjusted with sodium hydroxide (NaOH, pH 9.0) were used, preparing such solutions as foreseen in the statistical design in concentrations of 0.05, 0.10 and 0.15 mol L^{-1}, respectively, according to the methodology described by Molinari [29]. After the end of the procedure, the organo-clay carrier was filtered from the system and washed with distilled water to eliminate traces of non-adsorbed enzyme for later determination of its catalytic activity.

The enzymatic activity of the biocatalysts was performed via hydrolysis lipolytic activity, using a methodology adapted from Ferretti et al. [9]. Initially, an emulsion composed of a buffer solution of 50 mM sodium phosphate (pH 7.0), 10 wt% gum Arabic, and ROO (7.15%, m·vol^{-1}) was prepared, correcting the pH of the system when needed to 7.0 by adding a 50 mM NaOH solution. Subsequently, 20 mL of the emulsion with 0.5 mL of the sample of the enzymatic solution was added to the flask under constant agitation (20 min and 35 °C). To finalize the reaction, 20 mL of acetone:ethanol solution (1:1, vol.) was added, where the system was titrated with a 50 mM NaOH solution in the presence of phenolphthalein to determine the catalyst activity.

Enzymatic glycerolysis

To evaluate the catalytic activity of the newly immobilized enzyme in the glycerolysis reaction, another CCRD ($2^k + 2{\cdot}k$ with three repetitions at the central point) was used, seeking to optimize the reaction conditions that maximize the production of MAG and DAG. As independent variables, the effects of reaction temperature (x_3, ranging from 28.0 to 42.0 °C with the center point at 35.0 °C) and catalyst concentration (x_4, ranging from 3.97 to 11.02 vol.% with the center point at 7.50 vol.%)—according to proposed by Finco et al. [13]—was assessed in terms of TAG conversion (dependent variable, Z, %) to MAG and DAG. The reactions were performed in a jacketed glass batch reactor equipped with a temperature controller, where from preliminary tests, a glycerol to feedstock molar ratio of 2:1 and a reaction time of 2 h were defined to be used in the experiments. It is important to describe that the choice of the molar ratio between glycerol and oil also considered the minimization of inhibitory effects of alcohol on the enzyme, where typically molar ratios higher than 6:1 impair de TAG conversion since the hydrophilic glycerol wraps the surface of lipase, hindering the enzyme-ROO complex formation [30]. Using the optimized parameters obtained experimentally, a one-reuse test of the biocatalyst in a new reaction was accomplished, where the immobilized enzyme recovered from the system by filtration was washed with 50 mL of *n*-hexane and dried between the batches. After the conclusions of the reactions, samples were collected to determine the TAG, DAG, and MAG contents.

Statistical analysis

By the analysis of variance (ANOVA), regression analysis, and plotting of contour curves, the optimal conditions that maximize the TAGs conversion of the ROO, as well as the effectiveness of the lipase immobilization, were determined using the software Statistica®, version 11.0 (Statsoft

Inc., Tulsa, USA), considering a significance level of 95% ($p < 0.05$).

Kinetic parameters

From the conditions that returned the best conversion results of the feedstock, tests were performed to evaluate the kinetics of the considered system (in this particular stage for a reaction time of 9 h/540 min). Using the well-established Ping-Pong Bi-Bi mechanism (Eqs. 1, 2, 3, 4, 5, and 6), in addition to considering the hydrolysis reactions involved (Eqs. 7, 8, 9, and 10), mathematical modeling was evaluated to estimate the kinetic parameters as well as the order of the reaction. In the kinetic mathematical modeling of the ROO glycerolysis reaction, the following elementary reactions were considered:

$$\mathrm{TAG} + \mathrm{E} \underset{\mathrm{K_{-1}}}{\overset{\mathrm{K_1}}{\rightleftarrows}} \mathrm{E-TAG} \tag{1}$$

$$\mathrm{E-TAG} \xrightarrow{\mathrm{K_2}} \mathrm{DAG} + \mathrm{E-FFA} \tag{2}$$

$$\mathrm{E-FFA} + \mathrm{G} \underset{\mathrm{K_{-3}}}{\overset{\mathrm{K_3}}{\rightleftarrows}} \mathrm{E-FFA-G} \tag{3}$$

$$\mathrm{E-FFA-G} \xrightarrow{\mathrm{K_4}} \mathrm{MAG} + \mathrm{E} \tag{4}$$

$$\mathrm{DAG} + \mathrm{E} \underset{\mathrm{K_{-5}}}{\overset{\mathrm{K_5}}{\rightleftarrows}} \mathrm{E-DAG} \tag{5}$$

$$\mathrm{E-DAG} \xrightarrow{\mathrm{K_6}} \mathrm{MAG} + \mathrm{E-FFA} \tag{6}$$

$$\mathrm{E-TAG} + \mathrm{W} \underset{\mathrm{K_{-7}}}{\overset{\mathrm{K_7}}{\rightleftarrows}} \mathrm{DAG} + \mathrm{FFA} + \mathrm{E} \tag{7}$$

$$\mathrm{E-DAG} + \mathrm{W} \underset{\mathrm{K_{-8}}}{\overset{\mathrm{K_8}}{\rightleftarrows}} \mathrm{MAG} + \mathrm{E} + \mathrm{FFA} \tag{8}$$

$$\mathrm{MAG} + \mathrm{E} \underset{\mathrm{K_{-9}}}{\overset{\mathrm{K_9}}{\rightleftarrows}} \mathrm{MAG-E} \tag{9}$$

$$\mathrm{E-MAG} \xrightarrow{\mathrm{K_{10}}} \mathrm{FFA} + \mathrm{E} + \mathrm{G} \tag{10}$$

From the elementary equations, the kinetic equations (Eqs. 11, 12, 13, 14, 15, 16, 17, 18, 19, and 20) was described:

$$r_1 = -\mathrm{K_1}\mathrm{C_{TAG}}(t)\mathrm{C_E}(t) + \mathrm{K_{-1}}\mathrm{C_{TAG-E}}(t) \tag{11}$$

$$r_2 = -\mathrm{K_2}\mathrm{C_{TAG-E}}(t) \tag{12}$$

$$r_3 = -\mathrm{K_3}\mathrm{C_{E-FFA}}(t)\mathrm{C_G}(t) + \mathrm{K_{-3}}\mathrm{C_{E-FFA-G}}(t) \tag{13}$$

$$r_4 = -\mathrm{K_4}\mathrm{C_{E-FFA-G}}(t) \tag{14}$$

$$r_5 = -\mathrm{K_5}\mathrm{C_{DAG}}(t)\mathrm{C_E}(t) + \mathrm{K_{-5}}\mathrm{C_{E-DAG}}(t) \tag{15}$$

$$r_6 = -\mathrm{K_6}\mathrm{C_{E-DAG}}(t) \tag{16}$$

$$r_7 = -\mathrm{K_7}\mathrm{C_{E-TAG}}\mathrm{C_w}(t) + \mathrm{K_{-7}}\mathrm{C_{DAG}}(t)\mathrm{C_{FFA}}(t)\mathrm{C_E}(t) \tag{17}$$

$$r_8 = -\mathrm{K_8}\mathrm{C_{E-DAG}}\mathrm{C_w}(t) + \mathrm{K_{-7}}\mathrm{C_{MAG}}(t)\mathrm{C_{FFA}}(t)\mathrm{C_E}(t) \tag{18}$$

$$r_9 = -\mathrm{K_9}\mathrm{C_{MAG}}(t)\mathrm{C_E}(t) + \mathrm{K_{-9}}\mathrm{C_{E-MAG}}(t) \tag{19}$$

$$r_{10} = -\mathrm{K_{10}}\mathrm{C_{E-MAG}}(t)\mathrm{C_E}(t) + \mathrm{K_{-10}}\mathrm{C_{FFA}}(t)\mathrm{C_E}(t)\mathrm{C_G}(t) \tag{20}$$

Applying a molar balance for each species and considering the productivity based on reaction stoichiometry, the enzymatic kinetics model was obtained for the species involved in the reaction mechanism of glycerolysis, as described by Eqs. 21, 22, 23, 24, 25, 26, 27, 28, 29, 30, and 31):

$$\frac{\mathrm{dC_{TAG}}}{\mathrm{dt}} = r_1 \tag{21}$$

$$\frac{\mathrm{dC_{DAG}}}{\mathrm{dt}} = -r_2 + r_5 - r_7 \tag{22}$$

$$\frac{\mathrm{dC_{MAG}}}{\mathrm{dt}} = -r_4 - r_6 - r_8 + r_9 \tag{23}$$

$$\frac{\mathrm{dC_G}}{\mathrm{dt}} = -r_3 + r_{10} \tag{24}$$

$$\frac{\mathrm{dC_E}}{\mathrm{dt}} = r_1 - r_4 + r_5 - r_7 - r_8 + r_9 - r_{10} \tag{25}$$

$$\frac{\mathrm{dC_{E-TAG}}}{\mathrm{dt}} = -r_1 + r_2 + r_7 \tag{26}$$

$$\frac{\mathrm{dC_{E-FFA}}}{\mathrm{dt}} = -r_2 + r_3 - r_6 \tag{27}$$

$$\frac{\mathrm{dC_{E-FFA-G}}}{\mathrm{dt}} = -r_3 + r_4 \tag{28}$$

$$\frac{dC_W}{dt} = r_7 + r_8 \quad (29)$$

$$\frac{dC_{FFA}}{dt} = -r_7 - r_8 - r_{10} \quad (30)$$

$$\frac{dC_{MG-E}}{dt} = -r_9 + r_{10} \quad (31)$$

The mass balance for the free enzyme concentration was based on the concentrations of enzyme–substrate complexes, considering that the total enzyme concentration remained constant in the system, as represented by Eq. (32):

$$C_E(t=0) = C_E + C_{E-TAG} + C_{E-DAG} - C_{E-MAG} + C_{E-FFA} + C_{E-FFA-G} \quad (32)$$

The initial conditions are presented by Eqs. 33, 34, 35, 36, 37, 38, 39, 40, 41, 42, 43, and 44, where all concentration values are expressed in mol·L^1 and were calculated for each component based on the molecular mass of the ROO, the mass of each component, and the total mass of oil plus water:

$$C_{TAG}(0) = C_{TAG,0}^{exp} \quad (33)$$

$$C_{DAG}(0) = 0 \quad (34)$$

$$C_{MAG}(0) = 0 \quad (35)$$

$$C_G(0) = 0 \quad (36)$$

$$C_E(0) = C_{E,0}^{exp} \quad (37)$$

$$C_{E-TAG}(0) = 0 \quad (38)$$

$$C_{E-FFA}(0) = 0 \quad (39)$$

$$C_{E-FFA-G}(0) = 0 \quad (40)$$

$$C_W(0) = C_{W,0}^{exp} \quad (41)$$

$$C_{FFA}(0) = 0 \quad (42)$$

$$C_{E-MAG}(0) = 0 \quad (43)$$

$$C_{E-DAG}(0) = 0 \quad (44)$$

The parameters of the mathematical model (K_1, K_{-1}, K_2, K_3, K_{-3}, K_4, K_5, K_{-5}, K_6, K_7, K_{-7}, K_8, K_{-8}, K_9, K_{-9}, K_{10} e K_{-10}) were estimated from the experimental data of the enzymatic hydrolysis kinetics of ROO and the minimization of the objective function represented by Eq. (31). The Downhill simplex optimization method (Eq. 45) developed by Nelder and Mead [31] was used in the search for the minimum of the objective function. To solve the mathematical model, the numerical method of Rosenbrock [32] was used, using Maple® software (version 13, Waterloo Maple Inc., Canada).

$$ob = \sum_{j=1}^{nc}\sum_{i=1}^{nd}\left(C_{ji}^{exp} - C_{ji}^{mod}\right)^2 \quad (45)$$

where nc= number of components (TAG, DAG, MAG e FFA); nd= number of experimental data; C_{ji}^{exp}= experimental concentration of the component j and; C_{ji}^{mod}= concentration of the component j calculated by the model.

HPLC analysis

The quantification of TAG, DAG, and MAG was performed according to the methodology proposed by Finco et al. [13], using an HPLC (Thermo Scientific Ultimate 3000) equipped with a Phenomenex C18 chromatographic column of 5 µm and 100 Å (250×4,6 mm, model 00G-4252-E0), oven temperature of 35º, detector temperature 40 ºC, and injection volume of 20 µL with a flow rate of 1 mL·min^{-1} (mobile phase of acetonitrile:acetone, 1:1 vol./vol.).

The organo-clay carrier

The structural characterization of the clay support before and after immobilization (using the material obtained at the central point of the statistical design described in section "Enzymatic glycerolysis") was performed by transmission electron microscopy—TEM (Jeol JEM-1400), scanning electron microscopy—SEM (Shimadzu SperScan SS550) and Fourier transform infrared spectroscopy—FTIR (Bruker Vertex 70, in the wavelength range of 3000 to 300 cm^{-1} and with potassium bromide as reference with 100% of transmittance). Finally, X-Ray diffraction (XRD) was performed with a Shimadzu diffractometer (model XRD 6000) with Cu tube and Ni, Cu-Kα radiation (1.54 Å) at 40 kV at 30 mA from 2θ = 5° to 80°, scanning speed of 2.0º min^{-1}, and scanning step size of 0.02°. The interplanar distance was calculated based in Bragg's Law, according to Eq. (46):

$$n\,\lambda = 2d_{100}\text{sen}(\theta) \quad (46)$$

where λ is the wavelength of the radiation Cu-Kα (1.54 Å), n is the refractive index of the air (considered as 1.o), d_{100} is the interplanar distance, and θ the Bragg angle.

Results and discussion

Carrier characterization

To analyze the clayey material used as the support for the biocatalyst immobilization used in the glycerolysis reactions, TEM, SEM, and FTIR analyses were accomplished to investigate the interactions verified between enzyme and support. Figure 1 presents micrographs obtained through TEM analysis for the commercial clayey support Spectrogel® before and after its pretreatment with ternary salt. From the images, it is possible to verify that the material has a structure of interspersed layers, where the dark lines indicate the thickness of lamellae, which when together are spaced apart by the interplanar distance of the material [33]. Individual visualization is facilitated when there is exfoliation, that is, there is a lamellae dispersion. Analyzing Fig. 1, it is also possible to verify that there were no significant modifications after the pre-treatment of the clayey material, where it is only possible to observe some subparallel points and layer termination, demonstrating that the procedure does not damage the material's structure.

Figure 2 presents SEM images for clayey carrier Spectrogel® type C before and after the pretreatment and at 1000 × and 5000 × magnifications. From this image, it is possible to observe some irregularity in the surface of the particles as well as in their sizes. This characteristic is associated with the formation of agglomerates related to the stacking of octahedral layers of clayey minerals [34]. Another justification may be related to the addition of surfactant salts applied in the preparation of organophilic soils, where de Paiva et al. [35] report that the intercalation process of clayey compounds with quaternary salts increases the tendency to form agglomerates. Such features show solids formed by non-rigid aggregates of plate-shaped particles, evidencing the existence of mesopores. The image comparison of the material before and after treatment indicates that the procedure did not affect the structure of the clayey material, as no significant alterations were observed in the particles' morphology.

The FTIR technique was applied to identify the functional groups present in the clayey support samples before and after the pre-treatment procedure as well as after the reaction process. Through Fig. 3, it is possible to verify that the main characteristic bands of the material are at 3632 cm^{-1}, related to the O–H stretching of the water adsorbed on the clay structure, where the bands at 3446 and 1641 cm^{-1} indicate the H–O–H angular deformation between the layers of the clayey material [34, 36]. At 1021 cm^{-1}, an elongation of silicon-oxygen bonds (Si–O) is observed, at 913 and 793 cm^{-1} an angular variant of the O–H group is observed, and bands 722 and 467 cm^{-1} also refer to the phyllosilicate structure with Si–O and Si–O–Al angular deformation [36]. In the sections at 2923 and 2852 cm^{-1}, a symmetric and asymmetric elongation is observed, respectively, related to the vibrational elongations of the C–H bond, where according to Manzotti and dos Santos [34], they are associated with the organic components promoted by the quarternary salt

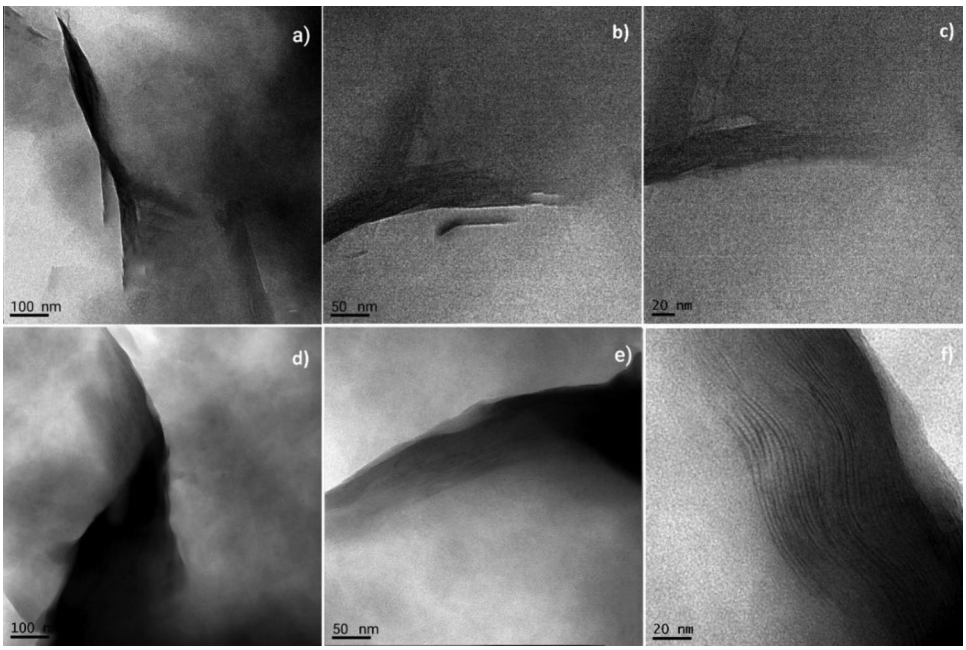

Fig. 1 Micrograph obtained by transmission electron microscopy for the commercial clay Spectrogel.® type C before (**a**–**c**) and after the pre-treatment (**d**–**f**)

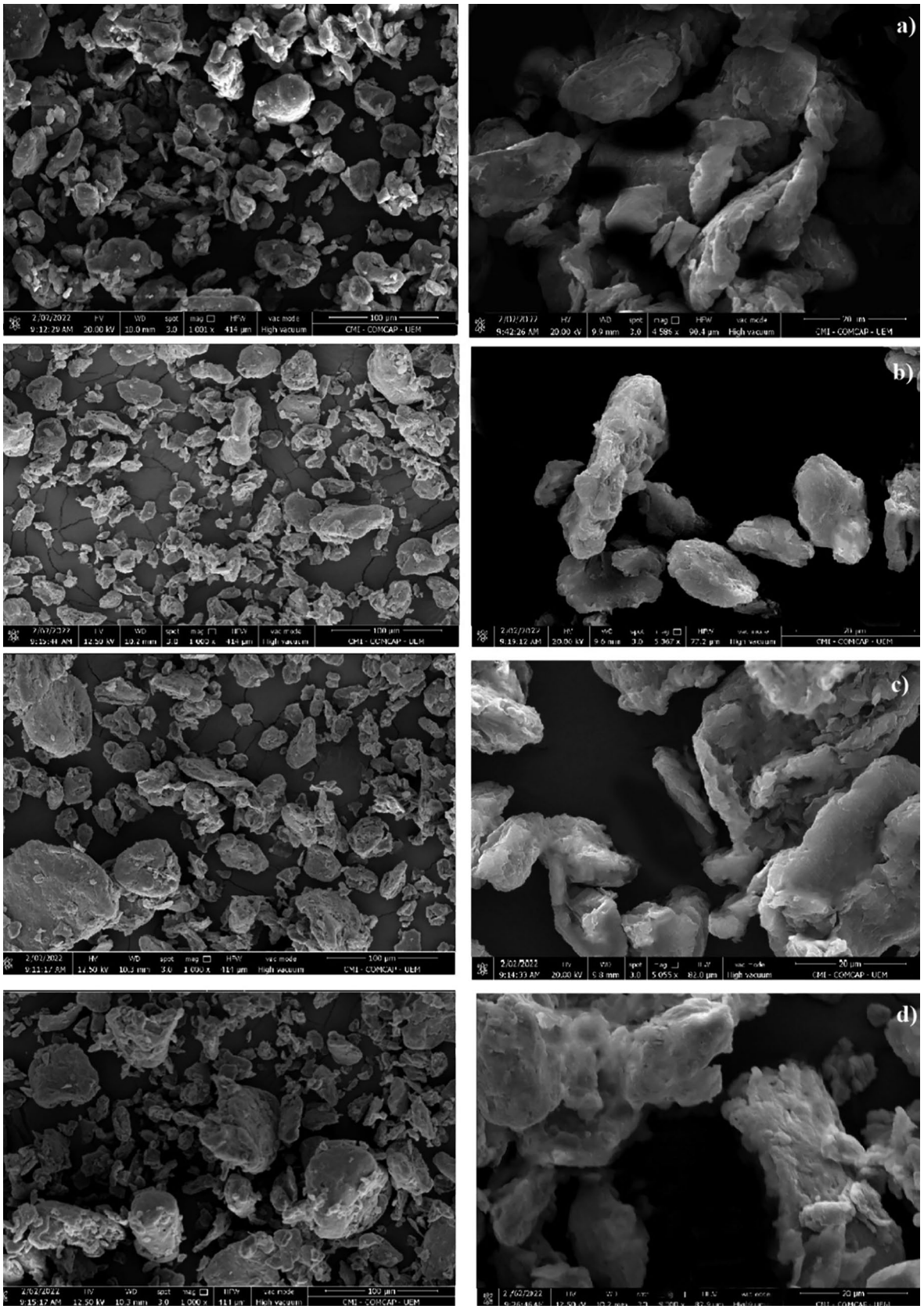

Fig. 2 Micrograph obtained by scanning electron microscopy for the clayey support Spectrogel.® type C before (**a**), after pretreatment (**b** and **c**), and with magnifications of 1000 × and 5000 × (**d**)

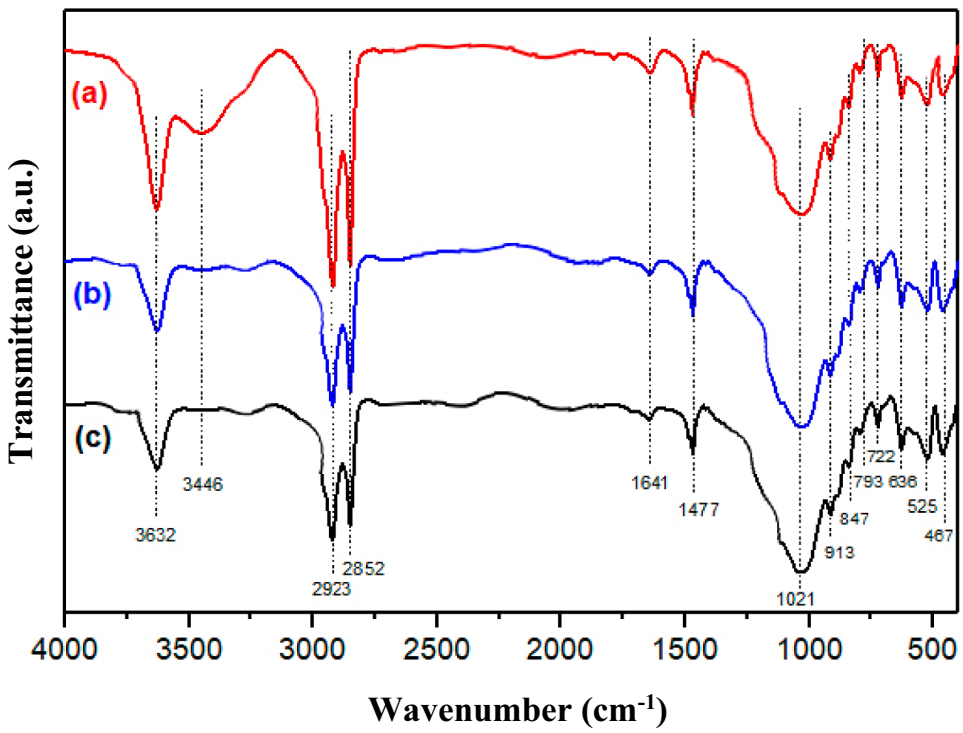

Fig. 3 FTIR spectra for the Spectrogel.® type C clay support before (**a**) and after pretreatment (**b**) as well as after the enzymatic glycerolysis reaction (**c**)

used in the pre-treatment of organophilization of the clayey support. In turn, the 1477 cm^{-1} band also signals the angular deformation of these groups (C–H) [36].

The most perceptible alteration in the structure of the clayey material is in the range of 3446 cm^{-1}, which refers to a reduction in the H–O–H band, representing the water present between the layers of clay after the reaction process. The band at 2923 cm^{-1} observed in the analyzed samples also refers to the vibrational stretching C–H of the CH_2 group [37]. It is also possible to observe a band at 2852 cm^{-1}, characteristic of the C–H group and the –CHO group. When analyzing the peak at 1.641 cm^{-1} of the C = N vibrational stretching, it is verified that it slightly increased regarding the sample before the glycerolysis reaction, a fact associated with the reaction process that occurred on the material surface [38]. Therefore, it is possible to perceive that the reaction promoted some modifications on the surface of the clayey support used to immobilize the lipase applied as a biocatalyst in the enzymatic glycerolysis.

Figure 4 presents the XRD patterns for the Spectrogel® type C carrier before and after pretreatment (activation) as well as after being used in the glycerolysis reaction. Through the image, it is possible to verify that the clayey material does not have a highly crystalline structure, a typical characteristic of these compounds. The basal interlayer space of the clayey material is $d_{001} = 1.27$ nm, suggesting that the intercalated carrier cations are arranged in monolayers, a usual data reported by other studies that used Spectrogel® type C for different purposes [36, 39]. After the activation and reaction steps where the lipase was adsorbed in its structure, the basal spacing was slightly shifted to 1.25 and 1.28 nm, respectively, indicating that both processes did not substantially affect the crystallinity of the clayey material, where the immobilization of the biocatalyst was delimited to the mineral surface. It is also interesting to verify in the XRD diffractogram the peaks detected at 0.197 and 0.283 nm, corresponding to quartz, which are typically weakly bound and ended up being displaced after the activation and reaction processes. Finally, the peaks detected at 0.335–0.336 nm are also associated with quartz, while the peaks between 0.442 and 0.449 are associated to the presence of montmorillonite, while the peaks at 0.150 nm, with an interplanar distance of d_{060}, are characteristic of materials with an octahedral structure [36].

Lipase immobilization assays

An experimental model for the enzymatic activity of Lipozyme® TL 100L immobilized on the Spectrogel® type C clay support was built according to the effects of the pH of the medium and the lipase load used, based on the coded variables is presented in Eq. (47), where positive coefficients indicate a synergy between the dependent variables and the response variable and negative coefficients suggest an adverse effect between the dependent variables and the response variable. Through this regression, it was possible to obtain the predicted values to compare with the results obtained experimentally in the circumstances considered, as presented in Table 1.

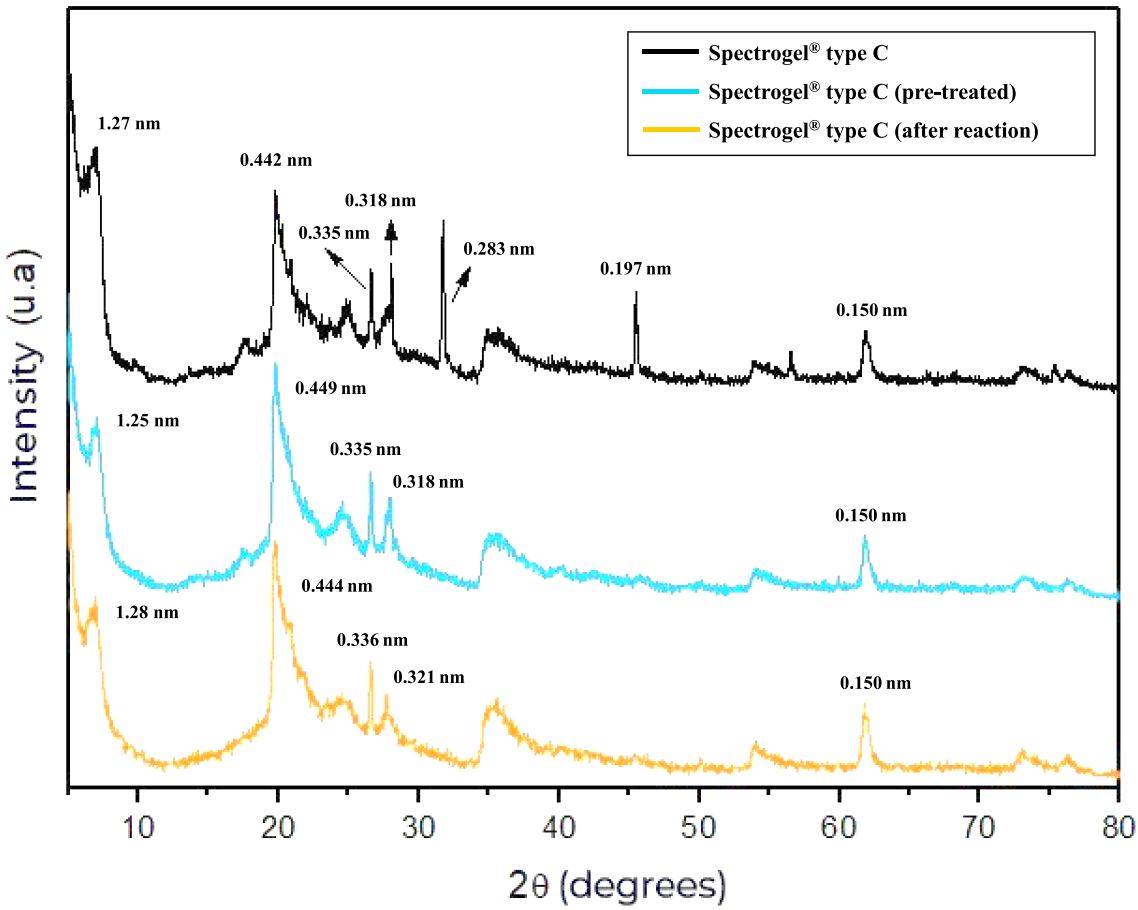

Fig. 4 XRD patterns of Spectrogel® type C before and after the pretreatment step as well as after the glycerolysis reaction

$$Y = 103.335 + 4.741x_1 - 31.310x_1^2 + 21.136x_2 - 11.133x_2^2 + 0.952x_1x_2 \quad (47)$$

where Y represents the enzymatic activity of the biocatalyst after immobilization, x_1 is the pH of the medium, and x_2 is the lipase load used in the assay.

Through an ANOVA, the statistical legitimacy of the proposed model can be evaluated, verifying the fit and significance of the regression proposed in Eq. (47), according to the data presented in Table 2. Considering the coefficient of determination obtained, 0.9742, it can be mentioned that an excellent fit of the data to the quadratic model was reached since 97.42% of the variability of the results can be justified by the regression as well as by the fact that they are associated with the independent variable. In addition, the low value for the coefficient of variation of the results (CV = 5.45%) indicates good reliability and precision of the experiments, since usually a CV < 10.0% suggests that the obtained model can be considered reproducible. Also, it is important to describe the proven significance for the quadratic model considering the results

Table 1 Conditions investigated in the immobilization process and the lipase activity of the immobilized enzyme obtained experimentally and predicted by the proposed model

Assay	Independent variables		Dependent variable	
	pH, x_1	Lipase load ($U \cdot g^{-1}$), x_2	Lipase activity ($U \cdot g^{-1}$), Y	Lipase activity (predicted, $U \cdot g^{-1}$), Y
1	5.0 (−1)	80 (−1)	44.80	35.97
2	9.0 (+1)	80 (−1)	48.99	43.54
3	5.0 (−1)	160 (+1)	79.12	76.33
4	9.0 (+1)	160 (+1)	87.12	87.72
5	3.3 (−1.41)	130 (0)	27.86	34.40
6	10.7 (+1,41)	130 (0)	46.03	47.77
7	7.0 (0)	64 (−1.41)	42.97	51.40
8	7.0 (0)	195 (+1,41)	111.15	111.00
9	7.0 (0)	130 (0)	101.40	103.33
10	7.0 (0)	130 (0)	103.25	103.33
11	7.0 (0)	130 (0)	105.46	103.33

Table 2 ANOVA to the effect of pH and lipase load in the immobilized enzyme activity

	Sum of squares	Degrees of freedom	Mean square	F_{calc}	F_{tab}
Regression	9932.65	5	1986.53	41.22	5.05
Residual	240.98	5	48.20		
Total	9503.91	10			

CV: 5.45%; Standard deviation: 3.966; R^2: 0.9746

obtained from the F-test, where a F_{calc} of 41.22 (more than 8 times higher than the F_{tab}) was obtained, indicating with a confidence level of 95% that the model has statistical meaning, being allowed to use it to predict the lipase activity after the immobilization process within the range of parameters considered.

Figure 5 presents a Pareto Diagram that allows analyzing the effects of independent variables on the enzymatic activity of the immobilized biocatalyst. Both quadratic terms of the variables "pH" and "lipase load" showed a negative effect on the response variable, while the linear term of the variable "lipase load" presented a positive effect on the response variable. A discussion regarding the reasons for such results obtained can be better visualized when it is analyzed the contour curve generated through the proposed model (Fig. 6), which demonstrates the influence of the pH of the medium and the lipase load on the activity of the immobilized enzyme. Through the results presented in Fig. 6, it is possible to verify that the highest enzymatic activities of the immobilized biocatalyst were obtained for a pH close to neutrality, ranging from 101.4 to 111.2 U g^{-1}. Distinct enzymes exhibit optimal stability and activity at or near their native pH, which is often close to neutral, including the lipases from *Thermomyces lanuginosus* fungus [40, 41]. Operating at the enzyme's optimal pH can help maintain its structural integrity and prevent episodes of denaturation. Therefore, immobilizing enzymes at a pH close to their natural range can preserve their stability and functionality. Moreover, neutral pH is generally more compatible with the stability and activity of other biomolecules, such as proteins or cofactors, that may be involved in the enzymatic immobilization process [42]. By avoiding extreme pH conditions, the risk of damaging these biomolecules and compromising the overall effectiveness of the immobilization process is minimized. Regarding the lipase load used in the experiments, a higher concentration of enzyme available to the adsorptive process tends to direct higher values of enzymatic activity, since a higher amount of biocatalyst available in the process will increase the chances of more lipase being adsorbed by the clayey support, although there is a limitation where adding more enzyme to the immobilization process does not affect the enzymatic activity of the lipase once the adsorptive capacity of the support has already achieved its load capacity. A similar observation was reported by Silva et al. [41], which investigated the immobilization of the *Thermomyces lanuginosus* lipase on a hydrophobic resin (Streamline phenyl™), where lipase loads higher than 14 mg g^{-1} (421.6 U g^{-1}) did not affect the enzyme activity of the biocatalyst, which already achieved its load capacity.

Using Eq. (47), the optimal condition for enzyme immobilization was determined: lipase load of 170.9 U g^{-1} (or 0.049 g of enzyme per g of support) and pH of 7.1. In this condition, experiments were performed in triplicate

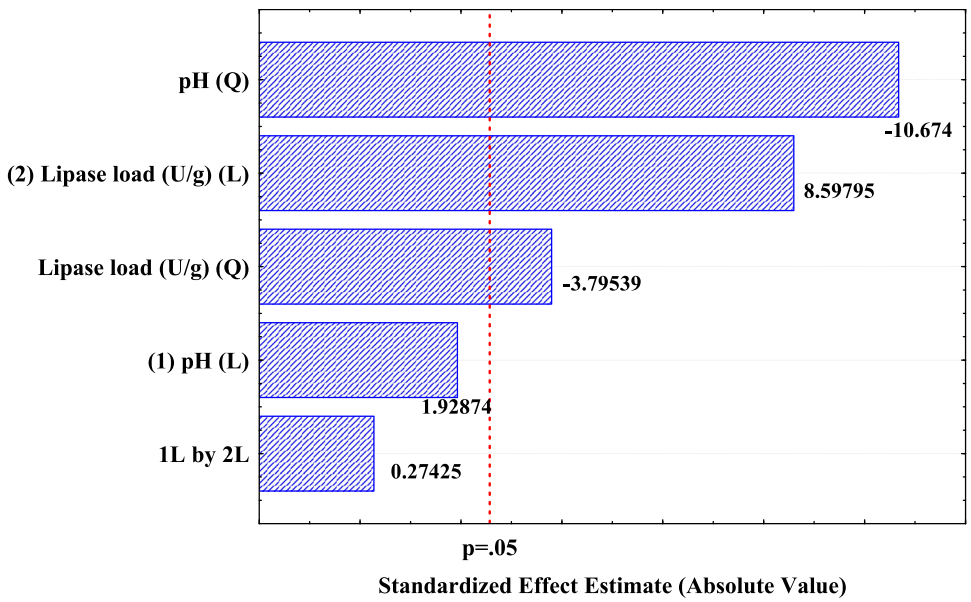

Fig. 5 Pareto chart of the effects of pH and lipase load in the immobilized enzyme activity

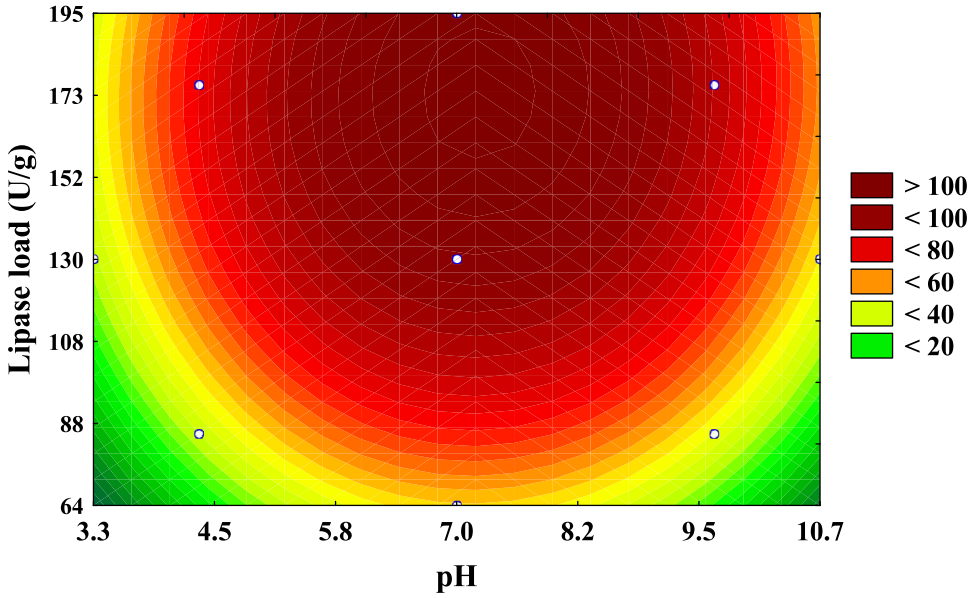

Fig. 6 Response of immobilized enzyme activity according to the variation of pH and lipase load in the medium

that returned an enzymatic activity of 93.2 ± 0.7 U g^{-1}, while the model returned a value of 96.1 U g^{-1}, a deviation of only 3.0% between the experimental value and the predicted data.

ROO glycerolysis

Process optimization

Similar to what was performed to determine the best conditions for immobilization of Lipozyme® TL 100L lipase, a new statistical design was carried out to evaluate the effects of reaction temperature (x_3) and biocatalyst concentration (x_4) on the conversion of triglycerides of the considered substrate (Z). Through the results obtained, it was possible to propose a model that represents such data, as shown in Eq. (48), based on the independent variables in their coded form. Table 3 shows the values predicted by this model in addition to the values obtained in the experiments.

$$Z = 95.159 + 6.514x_3 - 16.260x_3^2 + 3.004x_4 - 7.611x_4^2 - 1.0775x_3x_4 \quad (48)$$

The statistical acceptability of the model was evaluated through an ANOVA, according to the data presented in Table 4. Considering the coefficient of determination obtained of 0.8919, it is possible to observe the good fit of the data to the quadratic model, where 89.19% of the variability of the results are justified by the regression and they are linked to the independent variable. Moreover, the value CV = 11.77% also suggests an interesting reliability and precision of the experiments. Regarding the F-test, it was obtained an F_{calc} of 9.51, almost 2 times higher than the F_{tab}, indicating with a confidence level of 95% that the model

Table 3 Conditions investigated in the enzymatic glycerolysis and the triglycerides conversion obtained experimentally and predicted by the proposed model

	Independent Variables		Dependent Variable	
Assay	Temperature (°C), x_3	Lipase Conc (vol.%), x_4	Conversion (%), Z	Conversion (predicted, %), Z
1	30 (−1)	5.00 (−1)	56.52	60.69
2	40 (+1)	5.00 (−1)	71.14	75.88
3	30 (−1)	10.00 (+1)	62.93	68.86
4	40 (+1)	10.00 (+1)	73.24	79.73
5	28 (−1.41)	7.50 (0)	58.61	53.65
6	42 (+1.41)	7.50 (0)	77.78	72.02
7	35 (0)	3.97 (−1.41)	79.91	75.79
8	35 (0)	11.02 (+1.41)	90.87	84.26
9	35 (0)	7.50 (0)	94.88	95.16
10	35 (0)	7.50 (0)	95.68	96.16
11	35 (0)	7.50 (0)	94.79	95.16

Table 4 ANOVA to the effect of temperature and lipase concentration in the triglycerides conversion activity

	Sum of Squares	Degrees of Freedom	Mean Square	F_{calc}	F_{tab}
Regression	2220.68	5	444.14	9.41	5.05
Residual	235.97	5	47.19		
Total	2182.69	10			

CV: 11.77%; Standard deviation: 9.161; R^2: 0.8919

has statistical meaning, allowing its application to predict the TAG conversion within the range of the independent parameters considered.

Figure 7 presents the Pareto chart to this statistical design, showing the strong influence of both the linear and quadratic term of the variable "temperature" on the conversion of the raw material, where only the quadratic term of the concentration of lipase added to the reaction showed significance and negative effect to the response variable. Through these indications, plotting a contour curve to these results (Fig. 8) allows visualizing the real influence of the reaction temperature and lipase concentration in the feedstock conversion. In general, the TAG conversion ranged between 56% and 95% (information best visualized by the data shown in Table 2). Through the information available in Fig. 8, it is possible to note that this wide variation in the conversion of TAGs' feedstock may be related to the complex characteristic of the reaction medium, involving an emulsion necessary to somehow keep the reaction medium stable. Of course, it is expected that the reaction temperature substantially affects the stability of the medium, interfering in the catalytic properties of the enzyme, since such a biocatalyst is a temperature-sensitive protein, where temperatures below the so-named "ideal or optimal value" reduce its catalytic capacity at the same time as temperatures above the optimal can cause its denaturation, a process well known to be irreversible [17, 43]. Still, by the analysis of Fig. 8, it is possible to verify that the highest conversions of the raw material were obtained around the central point of the statistical design (35 °C and 7.5 vol.% of biocatalyst), where a higher concentration of lipase in the medium did not considerably affect the conversions, results similar to reported by other researches that applied the Lipozyme® TL 100 in reactions of glycerolysis and hydrolysis [44–46]. In this context, based on the optimization of the model proposed by Eq. (48) and the data presented in Fig. 8 via statistical software, it was concluded that the optimal condition for converting ROO into DAG and MAG is 36.5 °C and 7.9 vol.% of enzyme, where triplicate tests returned an average conversion of 96.97 ± 0.53%, values close to those indicated by the model (95.36%). As a complementary result, Fig. S1 (supplementary material) presents a chromatogram identifying the retention times of MAGs, DAGs, and TAGs.

An interesting and more practical mode to analyze the data obtained from glycerolysis reactions is to consider the biocatalyst productivity in terms of the volume of products obtained per volume of catalyst used in the reaction. From this perspective, it is important to note the excellent productivity of the tests performed with the lowest catalyst

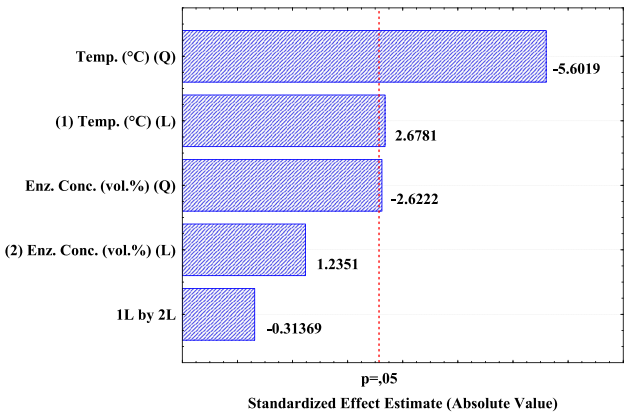

Fig. 7 Pareto chart of the effects of temperature and enzyme concentration on TAG conversion

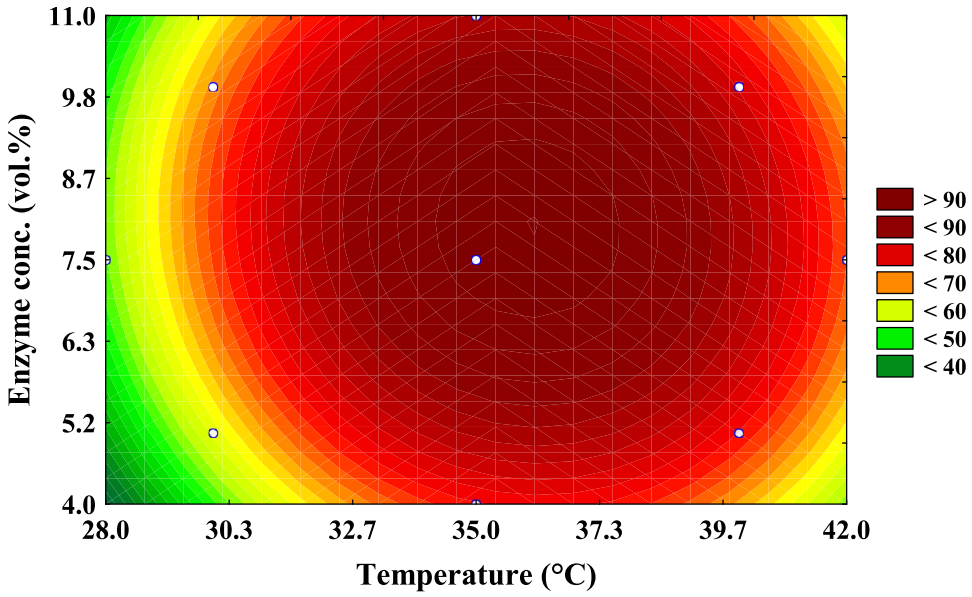

Fig. 8 Response of TAG conversion according to the variation of temperature and enzyme concentration in the reaction

load (3.97 vol.%), which returned 20.1 mL products (mL catalyst)$^{-1}$. The combination of 40 °C with 5.00 vol.% of enzyme also returned an interesting productivity of 14.2 mL products (mL catalyst)$^{-1}$, where reducing the reaction temperature to 30 °C decreased this value to 11.3 mL products (mL catalyst)$^{-1}$. Similar productivity was observed for the central point of statistical design: 12.7 mL products (mL catalyst)$^{-1}$ at 35 °C and 7.50 vol.% of lipase. On the other hand, the tests performed with 10.00 vol.% of immobilized lipase returned the lowest productivity observed: 6.3 and 7.3 mL products (mL catalyst)$^{-1}$ when a temperature of 30 and 40 °C was used in the reaction, respectively. Considering possible proposals to increase production scale and technical–economic evaluations, these data for biocatalyst productivity are important points to be considered.

Using the optimized condition for the glycerolysis test, a biocatalyst reuse assay was performed to evaluate its catalytic capacity in a new reaction. The experiments accomplished in triplicate returned a TAGs conversion of 81.47 ± 0.82%. Considering the conversion obtained for such experimental conditions in a first batch (96.97 ± 0.53%), a decrease in the feedstock conversion of approximately 15% was observed, an expected decline considering the possible issues that the lipase reuse could face, such as limited contact between substrate and enzyme caused by the adsorption of glycerol on the material surface, lipase leaching as well as its natural denaturation [22]. From another point of view, it can be concluded that the immobilized lipase maintained 85% of its initial efficiency, an important point considering economic aspects. For comparative purposes, such a result was not achieved by Molinari [29] when evaluating the immobilization of a lipase extracted from the *Burkholderia cepacia* microorganism in the Spectrogel® type C carrier, where after an initial efficiency of 98%, only 32% of Macauba oil conversion was reported after the first use of the biocatalyst, emphasizing the successful immobilization of the Lipozyme® TL 100 enzyme in the organo-clay support in the present research.

Kinetic data

From the optimized conditions for the reaction system considered (36.5 °C, 7.9 vol.% of Lipozyme® TL 100 immobilized on Spectrogel® type C, and a volumetric ratio between GLY:ROO of 2:1) the kinetic constants of the reaction were estimated, assuming the hypothesis of having a reaction coefficient as an independent factor in the medium. Such consideration is necessary since the use of excess enzyme in the reaction can result in its aggregation, exposing the active site of the biocatalyst to the substrate molecules, and making the model inefficient. The kinetic parameters for the elementary reactions involved (Eqs. 1, 2, 3, 4, 5, 6, 7, 8, 9, and 10) are presented in Table 5, where the results for the simulations are shown in Fig. 9, results very close to the experimental data. The experimental kinetic data show that the concentration of TAGs had a significant reduction in terms of concentration (accompanied by the formation of MAGs and DAGs) between times 0 and 120 min, indicating the effectiveness of the optimization of the parameters as well as the proposed model. Similar behavior was reported

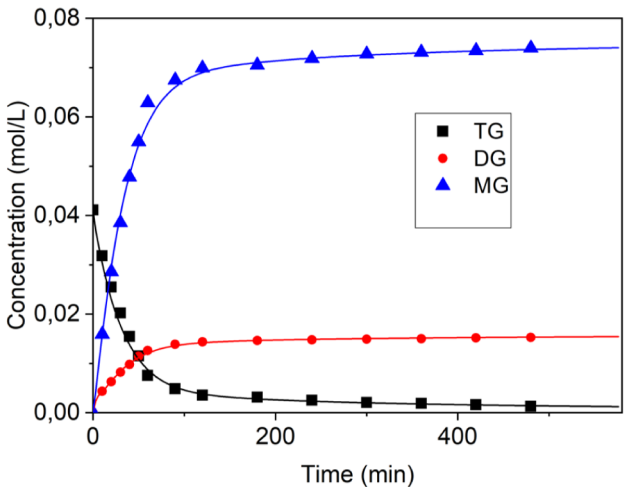

Fig. 9 Glycerolysis kinetics to the ROO. Reaction conditions: 36.5 °C, 7.9 vol.% of Lipozyme® TL 100 immobilized on Spectrogel® type C, volumetric ratio between GLY:ROO of 2:1, and 9 h

Table 5 Estimated kinetic constants for the glycerolysis reaction

Parameter	k_1 ($L \cdot g^{-1} \cdot min^{-1}$)	k_{-1} (min^{-1})	k_2 (min^{-1})	k_3 ($L \cdot mol^{-1} \cdot min^{-1}$)	k_{-3} (min^{-1})	k_4 (min^{-1})
Estimated Value	23.87	42.97	1.34	$1.01 \cdot 10^{9}$	$6.04 \cdot 10^{-8}$	$9.53 \cdot 10^{5}$
Parameter	k_5 ($L \cdot mol^{-1} \cdot min^{-1}$)	k_{-5} (min^{-1})	k_6 (min^{-1})	k_7 ($L \cdot mol^{-1} \cdot min^{-1}$)	k_{-7} ($L^2 \cdot g^{-1} \cdot mol^{-1} \cdot min^{-1}$)	k_8 ($L \cdot mol^{-1} \cdot min^{-1}$)
Estimated Value	9.82	10.44	15.22	0.88	18.07	$5.06 \cdot 10^{-9}$
Parameter	k_{-8} ($L^2 \cdot g^{-1} \cdot mol^{-1} \cdot min^{-1}$)	k_9 ($L \cdot mol^{-1} \cdot min^{-1}$)	k_{-9} ($L^2 \cdot g^{-1} mol^{-1} \cdot min^{-1}$)	k_{10} ($L \cdot mol^{-1} \cdot min^{-1}$)	k_{-10} ($L^2 \cdot g^{-1} \cdot mol^{-1} \cdot min^{-1}$)	
Estimated Value	226.96	3.65	6.13	289.98	212.34	

in the research of Corzo-Martínez et al. [47], which investigated the enzymatic glycerolysis of ratfish liver oil mediated by the Novozym® 435 lipase, indicating a higher formation of MAG and DAG in the first 120 min of reaction. Another important issue to be highlighted that can explain the good results reported in the present work can be associated with the adequate selection of parameters that resulted in the formation of a stable micellar system, an important factor for glycerolysis reactions.

With the aid of the Maple software, when analyzing the correlation coefficient between the theoretical model and experimental values obtained, the following coefficients were obtained: 0.9985 (to the MAGs), 0.9990 (to the DAGs), and 0.9972 (to the TAGs), indicating the excellent fit of the model.

Conclusions

This work reports experimental results regarding the immobilization of the commercial enzyme Lypozyme® TL 100L on the clay-based support Spectrogel® type C and its application as a biocatalyst of a glycerolysis reaction for the synthesis of mono- and diglycerides, where process parameters were evaluated as well as an estimate of kinetic constants of the reaction. The lipase load as well as the pH of the medium proved to be important factors in the enzyme immobilization process, where it was demonstrated the possibility of obtaining an enzyme with catalytic activity of 93.2 ± 0.7 U g^{-1}, using a lipase load of 170.9 U g^{-1} and pH of 7.1. Regarding the glycerolysis process mediated by the immobilized lipase, both the enzyme concentration and the reaction temperature proved to be significant factors for the process, where the optimization of these parameters via statistical model returned a feedstock conversion of 96.97 ± 0.53% at 36.5 °C and 7.9 vol.% of enzyme (for a GLY to ROO molar ratio of 2:1 and 2 h). Finally, the kinetic parameters of the elementary reactions involved in the process were determined, where through mathematical modeling, the comparison between experimental and theoretical data returned a fit higher than 0.99, demonstrating the excellent representation of the experimental data and reliability of the model proposed.

Supplementary Information The online version contains supplementary material available at https://doi.org/10.1007/s00449-024-02999-1.

Acknowledgements The authors are grateful for the scholarships of the Human Resources Program of the Brazilian Agency for Petroleum, Natural Gas and Biofuels—PRH/ANP through the Human Resources Training Program for Petroleum and Biofuels Processing and CAPES (Coordination for the Improvement of Higher Education Personnel, 001).

Author contributions **George F. Finco:** investigation; writing (original draft). **Edson A. da Silva:** conceptualization; validation, supervision. **Fernando Palú:** data curation; resources. **Márcia R. F. Klen:** conceptualization; resources. **Karina G. Fiametti:** writing (review and editing). **João H. C. Wancura:** writing (original draft), methodology. **J. Vladimir Oliveira:** formal analysis, writing (review and editing).

Funding The authors declare that no funds, grants, or other support were received during the preparation of this manuscript.

Data availability All data generated or analyzed during this study are included in this published article (and its supplementary information files).

Declarations

Conflict of interest The authors declare that they have no known competing financial interests or personal relationships that could have appeared to influence the work reported in this paper.

References

1. Li J, Guo R, Bi Y et al (2021) Comprehensive evaluation of saturated monoglycerides for the forming of oleogels. LWT 151:112061. https://doi.org/10.1016/j.lwt.2021.112061
2. Liu Z, Zhao M, Shehzad Q et al (2023) Whippable emulsions co-stabilized by protein particles and emulsifiers: the effect of emulsifier type. Food Hydrocoll 137:108379. https://doi.org/10.1016/j.foodhyd.2022.108379
3. Chen W, Liang G, Li X et al (2019) Impact of soy proteins, hydrolysates and monoglycerides at the oil/water interface in emulsions on interfacial properties and emulsion stability. Colloids Surfaces B Biointerfaces 177:550–558. https://doi.org/10.1016/j.colsurfb.2019.02.020
4. Arranz-Martínez P, Corzo-Martínez M, Vázquez L et al (2018) Lipase catalyzed glycerolysis of ratfish liver oil at stirred tank basket reactor: a kinetic approach. Process Biochem 64:38–45. https://doi.org/10.1016/j.procbio.2017.09.026
5. Hares Júnior SJ, Ract JNR, Gioielli LA, Vitolo M (2018) Conversion of triolein into mono- and diacylglycerols by immobilized lipase. Arab J Sci Eng 43:2247–2255. https://doi.org/10.1007/s13369-017-2635-7
6. Mouafo HT, Sokamte AT, Mbawala A et al (2022) Biosurfactants from lactic acid bacteria: a critical review on production, extraction, structural characterization and food application. Food Biosci 46:101598. https://doi.org/10.1016/j.fbio.2022.101598
7. Zhao X, Zhao F, Zhong N (2020) Production of diacylglycerols through glycerolysis with SBA-15 supported *Thermomyces lanuginosus* lipase as catalyst. J Sci Food Agric 100:1426–1435. https://doi.org/10.1002/jsfa.10140
8. Binhayeeding N, Klomklao S, Sangkharak K (2017) Utilization of waste glycerol from biodiesel process as a substrate for mono-, di-, and triacylglycerol production. Energy Procedia 138:895–900. https://doi.org/10.1016/j.egypro.2017.10.130
9. Ferretti CA, Spotti ML, Di Cosimo JI (2018) Diglyceride-rich oils from glycerolysis of edible vegetable oils. Catal Today 302:233–241. https://doi.org/10.1016/j.cattod.2017.04.008
10. Mamtani K, Shahbaz K, Farid MM (2021) Glycerolysis of free fatty acids: a review. Renew Sustain Energy Rev 137:110501. https://doi.org/10.1016/j.rser.2020.110501
11. Choong TSY, Yeoh CM, Phuah E-T et al (2018) Kinetic study of lipase-catalyzed glycerolysis of palm olein using Lipozyme TLIM in solvent-free system. PLoS One 13:e0192375

12. da Silva JAP, Bönmann VC, Kuamoto DT et al (2021) Glycerolysis of buriti oil (*Mauritia flexuosa*) by magnesium oxide and immobilized lipase catalysts: reaction yield and carotenoids degradation. J Am Oil Chem Soc 98:403–411. https://doi.org/10.1002/aocs.12469
13. Finco GF, Fiametti KG, Lobo VdS et al (2022) Kinetic study of liquid lipase-catalyzed glycerolysis of olive oil using Lipozyme <scp>TL 100L</scp>. J Am Oil Chem Soc 99:559–568. https://doi.org/10.1002/aocs.12593
14. Chen W, He L, Song W et al (2022) Encapsulation of lipases by nucleotide/metal ion coordination polymers: enzymatic properties and their applications in glycerolysis and esterification studies. J Sci Food Agric 102:4012–4024. https://doi.org/10.1002/jsfa.11749
15. Wang X, He L, Huang J, Zhong N (2021) Immobilization of lipases onto the halogen and haloalkanes modified SBA-15: enzymatic activity and glycerolysis performance study. Int J Biol Macromol 169:239–250. https://doi.org/10.1016/j.ijbiomac.2020.12.111
16. Santolin L, Fiametti KG, da Silva LV et al (2021) Enzymatic synthesis of eugenyl acetate from essential oil of clove using lipases in liquid formulation as biocatalyst. Appl Biochem Biotechnol 193:3512–3527. https://doi.org/10.1007/s12010-021-03610-z
17. Steinke G, Cavali M, Wancura JHC et al (2022) Lipase and phospholipase combination for biodiesel production from crude soybean oil. BioEnergy Res 15:1555–1567. https://doi.org/10.1007/s12155-021-10364-3
18. Li Y, Zhong N, Cheong L-Z et al (2018) Immobilization of *Candida antarctica* Lipase B onto organically-modified SBA-15 for efficient production of soybean-based mono and diacylglycerols. Int J Biol Macromol 120:886–895. https://doi.org/10.1016/j.ijbiomac.2018.08.155
19. An N, Zhou CH, Zhuang XY et al (2015) Immobilization of enzymes on clay minerals for biocatalysts and biosensors. Appl Clay Sci 114:283–296. https://doi.org/10.1016/j.clay.2015.05.029
20. Martin LS, Cerón AA, Molinari D et al (2019) Enhancement of lipase transesterification activity by immobilization on β–cyclodextrin-based polymer. J Sol-Gel Sci Technol 91:92–100. https://doi.org/10.1007/s10971-019-05011-5
21. de Farias MB, Spaolonzi MP, Silva MGC, Vieira MGA (2021) Fixed-bed adsorption of bisphenol A onto organoclay: characterisation, mathematical modelling and theoretical calculation of DFT-based chemical descriptors. J Environ Chem Eng 9:106103. https://doi.org/10.1016/j.jece.2021.106103
22. Wancura JHC, Brondani M, dos Santos MSN et al (2023) Demystifying the enzymatic biodiesel: how lipases are contributing to its technological advances. Renew Energy 216:119085. https://doi.org/10.1016/j.renene.2023.119085
23. Zhong N, Chen W, Liu L, Chen H (2019) Immobilization of *Rhizomucor miehei* lipase onto the organic functionalized SBA-15: their enzymatic properties and glycerolysis efficiencies for diacylglycerols production. Food Chem 271:739–746. https://doi.org/10.1016/j.foodchem.2018.07.185
24. Ketzer F, Wancura JHC, Tres MV, de Oliveira JV (2022) Kinetic and thermodynamic study of enzymatic hydroesterification mechanism to fatty acid methyl esters synthesis. Bioresour Technol 356:127335. https://doi.org/10.1016/j.biortech.2022.127335
25. Araki CA, Marcucci SMP, da Silva LS et al (2018) Effects of a combination of lipases immobilised on desilicated and thiol-modified ZSM-5 for the synthesis of ethyl esters from macauba pulp oil in a solvent-free system. Appl Catal A Gen 562:241–249. https://doi.org/10.1016/j.apcata.2018.06.007
26. Zhu R, Zhou Q, Zhu J et al (2015) Organo-clays as sorbents of hydrophobic organic contaminants: sorptive characteristics and approaches to enhancing sorption capacity. Clays Clay Miner 63:199–221. https://doi.org/10.1346/CCMN.2015.0630304
27. Dizge N, Keskinler B, Tanriseven A (2009) Biodiesel production from canola oil by using lipase immobilized onto hydrophobic microporous styrene–divinylbenzene copolymer. Biochem Eng J 44:220–225. https://doi.org/10.1016/j.bej.2008.12.008
28. Tran D-T, Chen C-L, Chang J-S (2012) Immobilization of Burkholderia sp. lipase on a ferric silica nanocomposite for biodiesel production. J Biotechnol 158:112–119. https://doi.org/10.1016/j.jbiotec.2012.01.018
29. Molinari D (2020) Immobilization of *Burkholderia cepacia* lipase in clay for application in the production of ethyl esters. State University of Maringá
30. Sun S, Wang G, Wang P (2018) A cleaner approach for biodegradable lubricants production by enzymatic glycerolysis of castor oil and kinetic analysis. J Clean Prod 188:530–535. https://doi.org/10.1016/j.jclepro.2018.04.015
31. Nelder JA, Mead R (1965) A simplex method for function minimization. Comput J 7:308–313. https://doi.org/10.1093/comjnl/7.4.308
32. Rosenbrock HH (1963) Some general implicit processes for the numerical solution of differential equations. Comput J 5:329–330. https://doi.org/10.1093/comjnl/5.4.329
33. Batista AH, Melo VF, Rate AW et al (2018) Scanning and transmission analytical electron microscopy (STEM-EDX) can identify structural forms of lead by mapping of clay crystals. Geoderma 310:191–200. https://doi.org/10.1016/j.geoderma.2017.09.026
34. Manzotti F, dos Santos OAA (2019) Evaluation of removal and adsorption of different herbicides on commercial organophilic clay. Chem Eng Commun 206:1515–1532. https://doi.org/10.1080/00986445.2019.1601626
35. de Paiva LB, Morales AR, Valenzuela Díaz FR (2008) Organoclays: properties, preparation and applications. Appl Clay Sci 42:8–24. https://doi.org/10.1016/j.clay.2008.02.006
36. Maia GS, de Andrade JR, da Silva MGC, Vieira MGA (2019) Adsorption of diclofenac sodium onto commercial organoclay: kinetic, equilibrium and thermodynamic study. Powder Technol 345:140–150. https://doi.org/10.1016/j.powtec.2018.12.097
37. Xue A, Zhou S, Zhao Y et al (2010) Adsorption of reactive dyes from aqueous solution by silylated palygorskite. Appl Clay Sci 48:638–640. https://doi.org/10.1016/j.clay.2010.03.011
38. Yiğitoğlu M, Temoçin Z (2010) Immobilization of *Candida rugosa* lipase on glutaraldehyde-activated polyester fiber and its application for hydrolysis of some vegetable oils. J Mol Catal B Enzym 66:130–135. https://doi.org/10.1016/j.molcatb.2010.04.007
39. de Andrade JR, Oliveira MF, Canevesi RLS et al (2020) Comparative adsorption of diclofenac sodium and losartan potassium in organophilic clay-packed fixed-bed: X-ray photoelectron spectroscopy characterization, experimental tests and theoretical study on DFT-based chemical descriptors. J Mol Liq 312:113427. https://doi.org/10.1016/j.molliq.2020.113427
40. Dixit M, Chhabra D, Shukla P (2023) Optimization of endoglucanase-lipase-amylase enzyme consortium from *Thermomyces lanuginosus* VAPS25 using multi-objective genetic algorithm and their bio-deinking applications. Bioresour Technol 370:128467. https://doi.org/10.1016/j.biortech.2022.128467
41. Silva JMF, dos Santos KP, dos Santos ES et al (2023) Immobilization of *Thermomyces lanuginosus* lipase on a new hydrophobic support (Streamline phenyl™): strategies to improve stability and reusability. Enzyme Microb Technol 163:110166. https://doi.org/10.1016/j.enzmictec.2022.110166
42. Qu P, Li D, Lazim R et al (2022) Improved thermostability of *Thermomyces lanuginosus* lipase by molecular dynamics simulation and in silico mutation prediction and its application in biodiesel production. Fuel 327:125039. https://doi.org/10.1016/j.fuel.2022.125039

43. Moya-Ramírez I, García-Román M, Fernández-Arteaga A (2016) Waste frying oil hydrolysis in a reverse micellar system. ACS Sustain Chem Eng 4:1025–1031. https://doi.org/10.1021/acssuschemeng.5b01118
44. Tu Q, Lu M, Knothe G (2017) Glycerolysis with crude glycerin as an alternative pretreatment for biodiesel production from grease trap waste: parametric study and energy analysis. J Clean Prod 162:504–511. https://doi.org/10.1016/j.jclepro.2017.06.064
45. Raizer E (2015) Use of ultrasound in diacylglycerol synthesis via enzymatic hydrolysis of sunflower oil. Western State University of Paraná, Toledo
46. Monte Blanco SFM, Santos JS, Feltes MMC et al (2015) Optimization of diacylglycerol production by glycerolysis of fish oil catalyzed by Lipozyme TL IM with Tween 65. Bioprocess Biosyst Eng 38:2379–2388. https://doi.org/10.1007/s00449-015-1473-9
47. Corzo-Martínez M, Vázquez L, Arranz-Martínez P et al (2016) Production of a bioactive lipid-based delivery system from ratfish liver oil by enzymatic glycerolysis. Food Bioprod Process 100:311–322. https://doi.org/10.1016/j.fbp.2016.08.003